Journal of Solid State Chemistry 183 (2010) 1245–1251

Contents lists available at ScienceDirect

Journal of Solid State Chemistry

journal homepage: www.elsevier.com/locate/jssc

Low temperature structural variations and molar heat capacity of stolzite, $PbWO_4$

Dmytro M. Trots [a,b,*], Anatoliy Senyshyn [c,d], Björn C. Schwarz [e]

[a] Bayerisches Geoinstitut, Universität Bayreuth, D-95440 Bayreuth, Germany
[b] Hamburger Synchrotronstrahlungslabor am Deutsches Elektronen-Synchrotron, Notkestr. 85, D-22607 Hamburg, Germany
[c] Fachbereich Materialwissenschaft, Technische Universität Darmstadt, Petersenstr. 23, D-64287 Darmstadt, Germany
[d] Forschungsneutronenquelle Heinz-Maier-Leibnitz (FRM II), Technische Universität München, Lichtenbergstr. 1, D-85747 Garching b. München, Germany
[e] Leibniz-Institut für Festkörper- und Werkstoffforschung Dresden (IFW Dresden), Institut für Komplexe Materialien, Helmholzstrasse 20, PF 270116, D-01171 Dresden, Germany

ARTICLE INFO

Article history:
Received 12 January 2010
Received in revised form
22 March 2010
Accepted 28 March 2010
Available online 2 April 2010

Keywords:
Lead tungstate
Scintillator material
Crystal structure
Thermal properties

ABSTRACT

The crystal structure, thermal expansion and heat capacity of $PbWO_4$ (mineral name stolzite) scintillator material were comprehensively studied over a wide temperature range. No phase transitions were found down to 2 K ($I4_1/a$, scheelite structure type). A distinct feature of the temperature induced structural variations in $PbWO_4$ are the different thermal elongations of shorter and longer Pb–O distances. The low-temperature thermal expansion of $PbWO_4$ was parameterized on the basis of the 1st order Grüneisen approximation using a Debye function for the internal energy with a Debye temperature of 237 K, a bulk modulus of 67 GPa and a Grüneisen parameter of 1.08. The expansion along the *c*-axis is about 2.5–3 times higher in the range 23–290 K than along the *a*-direction. This pronounced anisotropy of the thermal expansion arises from the arrangements of rigid tetrahedral WO_4^{2-} units along ⟨100⟩–directions while Pb^{2+} cations occupy the sites between WO_4^{2-} in ⟨001⟩–directions.

1. Introduction

Lead tungstate is implemented in a high precision electromagnetic calorimeters for particle detection in the GeV and TeV regions at the world's largest particle physics facilities [1–4]. $PbWO_4$ is a fast and dense scintillator with good radiation resistance, however, its light yield is low [1] and varies drastically with temperature above 170 K due to thermal quenching of luminescence [5,6]. Thus, in order to improve the performance of electromagnetic calorimeters, a temperature stability better than 0.1 K at 291 K [1] or a cooling down of the calorimeter's environment to around 248 K [3] is necessary.

Lead tungstate occurs in nature as the tetragonal mineral stolzite (scheelite structure-type, $I4_1/a$ symmetry) or the monoclinic raspite ($P2_1/a$ symmetry). The scheelite-type synthetic $PbWO_4$ is used in particle physics. Two lead deficient structures $Pb_7W_8O_{32-x}$ [7] and $Pb_{7.5}W_8O_{32}$ [8] crystallizing in $P4/nnc$ and $P\overline{4}$ symmetries were recently reported, while the existence of these lead deficient modifications of $PbWO_4$ was not confirmed in the work of Chipaux et al. [9] and no deviation from the scheeleite structure has been observed on specimens from different sources. In addition to diffraction experiments at ambient conditions, the structure of $PbWO_4$ has been investigated at 1.4 K in the latter paper: no phase transitions were revealed and the thermal expansion was estimated by linear approximation based on 290 and 1.4 K temperature points. According to [9], the values for the thermal expansion along the *a*- and *c*-axes are 6×10^{-6} and $17\times10^{-6}\,K^{-1}$, respectively. In Ref. [10], coefficients of the thermal expansion tensor were derived for five different temperature intervals between 100 and 800 K; anisotropy in expansivity was observed. Axial thermal expansion coefficients of $PbWO_4$ were calculated from (004) and (008) Bragg maxima along ⟨001⟩ and from (200) and (400) along ⟨100⟩ based on the nine temperature points [11]: average coefficients between 25 and 900 °C equal $\alpha_c=29.5(6)\times10^{-6}\,°C^{-1}$ and $\alpha_a=12.8(6)\times10^{-6}\,°C^{-1}$. A slow increase in the expansion coefficients with temperature, a large anisotropy of the thermal expansion($\alpha_c/\alpha_a\sim2.3$) and the necessity of small temperature gradients during growth for obtaining crack-free crystals were also discussed. Monotonic variations of the lattice parameters with thermal expansion coefficients $\alpha_c=27\times10^{-6}\,K^{-1}$ and $\alpha_a=11\times10^{-6}\,K^{-1}$ were reported for $PbWO_4$ between 293 and 823 K in [12].

Only limited information concerning the structural behaviour of lead tungstate in the cryogenic region is available: in Ref. [9], two data sets at 290 and 1.4 K were examined without any

* Corresponding author at: Bayerisches Geoinstitut, Universität Bayreuth, D-95440 Bayreuth, Germany.
E-mail addresses: d_trots@yahoo.com (D.M. Trots), Anatoliy.Senyshyn@frm2.tum.de (A. Senyshyn).

0022-4596/$ - see front matter © 2010 Elsevier Inc. All rights reserved.
doi:10.1016/j.jssc.2010.03.039

information concerning atomic displacement parameters or interatomic distances, whereas data analysis in [10] was restricted by the technique available at that time. Information on structure and thermal properties (i.e., thermal expansion and specific heat) is an extremely important issue with respect to increasing the light yield at low temperatures in addition to the possibility of using $PbWO_4$ scintillator in cryogenic environments. Thus, we report a detailed study of the structure of $PbWO_4$ and its thermal evolution in the range 3.5–298 K combined with a parametrization of the thermal expansion on the basis of a 1st order Grüneisen approximation with a Debye approximation for the internal energy. The isobaric heat capacity of $PbWO_4$ between 2.0 and 353.5 K is also presented for the first time.

2. Experimental

A commercially available $PbWO_4$ scintillator crystal was used for the diffraction and calorimetric experiments. Preliminary conventional X-ray diffraction measurements were performed on the powdered sample with Si as an internal standard using a STOE STADI P diffractometer (Cu$K\alpha_1$ radiation selected by a curved Ge (111) monochromator, θ–2θ transmission geometry, 2θ range 5–109.99° and step size 0.01°, curved position-sensitive detector). Neutron powder diffraction data were collected using the structure powder diffractometer SPODI [13] installed at the neutron research reactor FRM-II (Garching, Germany). The powdered sample was filled into a cylindrical can of 8 mm diameter, made from a thin (0.15 mm wall thickness) vanadium foil and mounted into the closed-cycle refrigerator. Thermal neutrons (wavelength of 1.5488 Å) were taken from the 155° take-off using a vertically focused Ge(551) composite monochromator. Eighteen diffraction patterns were collected over a 2θ range of 11 −148.9° in a steps of 0.04° at temperatures of 3.5–298 K. The full-profile Rietveld method was applied for the analysis of the neutron diffraction data using the FullProf suite of programs [14].

The constant pressure heat capacity was measured in the temperature range of 2.0–353.5 K during heating. A PPMS calorimeter (quantum design) operating via the relaxation principle with a temperature change of $\Delta T = 0.02$ T was used. A layer of Apiezon N and Apiezon H grease, applied between the sample platform and the flat crystal, supported the thermal relaxation in the temperature range of 2–300 and 300–353.5 K, respectively. A two time constant model was used to fit the measured data.

3. Results and discussion

3.1. Structural behaviour

The inspection of systematic absences of reflections in the powder diffraction patterns of $PbWO_4$ confirmed the tetragonal $I\,4_1/a$ symmetry and the initial Rietveld refinements were based on the scheelite structure model (see for instance [15]). Our results from X-ray powder diffraction on $PbWO_4$ with Si as an internal standard indicate the lattice parameters $a = 5.46320(2)$ Å and $c = 12.04821(8)$ Å at ambient conditions. The structural parameters of $PbWO_4$, as obtained from neutron powder diffraction data, are summarized in a supplementary data (supplementary files supplied are published online alongside the electronic version of this article in Elsevier Web products, including ScienceDirect: http://www.sciencedirect.com). The graphical representation of the quality of the Rietveld fit and the atom positions in the unit cell of the crystal are shown in Figs. 1 and 2, respectively. Four oxygen atoms are arranged around the tungsten in an isolated non-regular tetrahedron. The presence of the isolated WO_4 tetrahedra is a distinct feature of the scheelite structure that substantiates the use of a quasimolecular anion complex approximation for the interpretation of the physical properties of the crystal [15]. The bond between the Pb^{2+} and WO_4^{2-} anion is mainly ionic, whereas inside the WO_4 complex the W–O bonds are primarily covalent. The lead cation has a coordination number of eight with respect to oxygen. Each PbO_8 polyhedron shares edges with four neighboring PbO_8 polyhedra and share corners with eight adjacent WO_4 tetrahedra. Each tetrahedron is corner linked to eight PbO_8 polyhedra, i.e., each tetrahedral vertex is corner linked to two vertexes of the PbO_8 polyhedra. Each PbO_8 polyhedron has two types of distances: four shorter and four longer Pb–O equal distances, whereas the WO_4 tetrahedron adopts four equal W–O bonds. Moreover, open channels parallel to the a-axis are present in the structure (Fig. 2).

Selected distances and angles in the $PbWO_4$ structure are presented in Fig. 3. Obviously, the expansivity is dominated by the larger temperature dependencies of the Pb–O distances in comparison to the tiny temperature induced changes of the W–O lengths, because WO_4^{2-} behaves like a rigid and isolated tetrahedral unit. In particular, the W–O change in length from 1.7891(6) Å at 3.5 K to 1.7853(6) Å at 298 K ; the four shorter Pb–O lengths from the 8-fold oxygen environment of Pb increase from 2.5954(5) Å at 3.5 K to 2.6114(5) Å at 298 K, and the four longer ones from 2.6270(5) to 2.6378(5) Å. Indeed, there is some spurious decrease in W–O distances occurred upon heating which is related to the presence of correlated thermal motion of rigid WO_4-unit in stolzite. As it is mentioned in the number

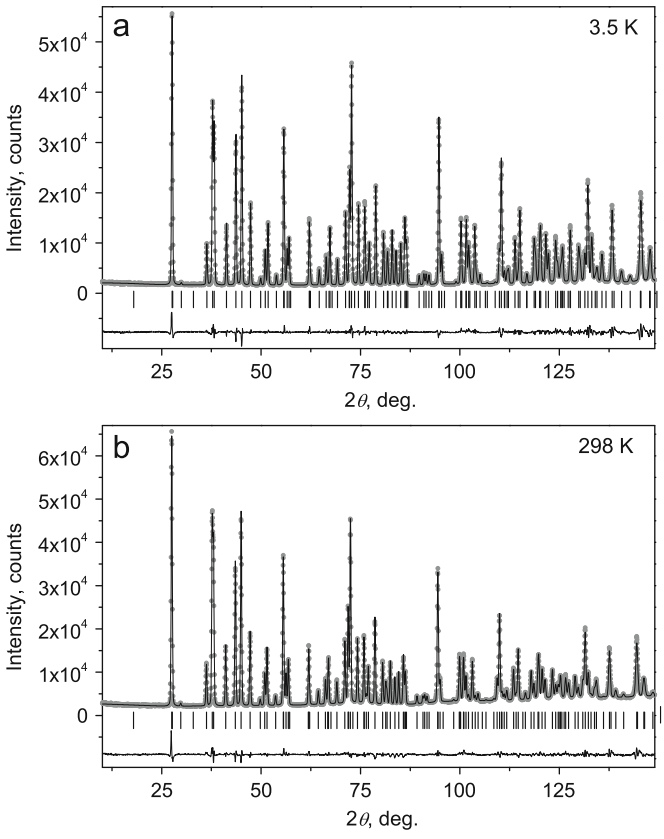

Fig. 1. Powder diffraction patterns with model profiles from Rietveld refinements at ambient conditions and 3.5 K. Points are experimental data, the line through the points represents the calculated profile and the curve at the bottom is the difference between experimental and calculated profiles. The vertical ticks show the calculated positions of the Bragg reflections.

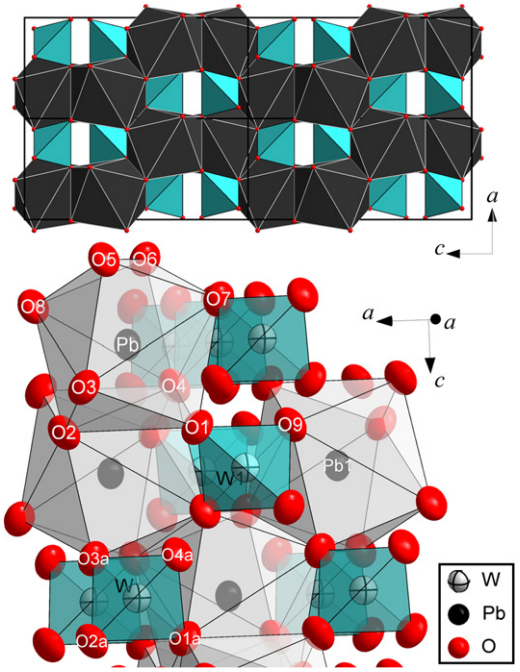

Fig. 2. (Color online) Graphical representation of the scheelite-structure of $PbWO_4$ in the (100) plane (above) and a structural fragment with the labeling scheme used for Fig. 3 and tables of structural parameters (see supplementary data).

of references (see for instance [16,17]), the volume of the rigid WO_4-unit is practically temperature independent for a number of scheelite-structure compounds, however, the correlated thermal motion can lead to an apparent reduction in bond length as a function of temperature [17]. Despite an estimation of contribution from thermal motion effects to W–O distances in $PbWO_4$ yields overall changes of about 0.0026 Å that fits into a range of 2 e.s.d., we corrected for clarity reasons W–O distances for correlated thermal motion of WO_4 rigid unit by method described in [18]. The variations of observed and thermally corrected W–O distances are shown in W–O vs. T plot in Fig. 3: no changes of corrected data over the whole temperature range is evident. All angles O–W–O within the tetrahedra and the smaller interpolyhedral angles W–O–Pb are practically temperature independent, whereas the larger interpolyhedral angles W–O–Pb increase significantly from 134.12(2)° at 3.5 K to 134.44(3)° at 298 K (Fig. 3). The PbO_8 (WO_4) polyhedral volumes change from 31.653 Å^3 (2.932 Å^3) at 3.5 K to 32.152 Å^3 (2.913 Å^3) at 298 K. These experimental findings are consistent with recent high-pressure diffraction studies on $PbWO_4$ [19,20]: the larger compressibility of the Pb–O distances in comparison to the W–O distances and the pressure induced changes of the intrapolyhedral W–O–Pb angles without any significant variation of the intratetrahedral O–W–O angles were confirmed.

It is interesting to note that in $PbWO_4$ the shorter Pb–O distances expand more strongly than the longer Pb–O distances (Fig. 3). According to our unpublished results [21,22], the same effect does not occur in $CaWO_4$ at least in the low temperature range. This reveals a principal difference in the temperature behaviour of the scheelite-type $PbWO_4$ and $CaWO_4$. Comparing the temperature induced changes to pressure induced structural variations in several scheelite-type compounds, practically similar compressibilities of the respective shorter and longer distances between oxygen and larger cations were observed in $PbWO_4$, $BaWO_4$ [19] and $CaWO_4$ [23]. However, distinct differences in the distortions of PbO_8 and BaO_8 polyhedra under pressure were observed by Grzechnik et al. [19], who initiated a discussion concerning the influence of the stereochemical activity of the non-bonding electron pair in the Pb^{2+} cation on the structural behaviour of $PbWO_4$. By analogy, the different expansivities of the shorter and longer distances in lead tungstate might probably be attributed to the existence of the Pb^{2+} ion in the structure, because the "nonbonded" lone-pair might influence the bonding (i.e., expansivity) in $PbWO_4$.

In 1985 Hazen investigated the high-pressure crystal chemistry of tungstates and molybdates: although no temperature dependent structure refinements were available at that time, the general aspects of structural variations for scheelite-type tungstates and molybdates were inferred from thermal expansion data [23]. Hence, this previous work reported that structural variations in the scheelite-type tungstates and molybdates have the same origin, whether they are caused by changes in temperature, pressure or composition. However, the work [19] and our investigation reveal deviations from Hazen's statement concerning the "analogous behaviour" of scheelite-type compounds because:

(a) $PbWO_4$ displays different expansivities of shorter and longer Pb–O distances, whereas the compressibilities of respective distances are the same;
(b) distinct pressure induced variations in PbO_8 and BaO_8 dodecahedra were observed in $PbWO_4$ and $BaWO_4$ [19].

However, it is impossible to draw more clear conclusions concerning the systematics/reasons of structural variations in scheelite-type tungstates and molybdates, because accurate structural information is still not available.

A thorough analysis of the observed displacement parameters requires a quantitative treatment, which can be performed using the method proposed by Lonsdale [24], where atomic displacement parameters B_{iso} can be described in the framework of the Debye model by the following relation:

$$B_{iso} = 8\pi^2\left[\frac{145.55T}{M}\left(\frac{k_B}{h\nu_D}\right)^2\varphi\left(\frac{\nu_D}{T}\right)+\frac{36.39k_B}{M h\nu_D}+B_{static}\right] \quad (1)$$

The phonon spectrum can be approximated by a parabolic function truncated at the maximum frequency ν_D, T is the temperature, k_B and h are Boltzmann and Plank constants, M is the atomic mass of the vibrating species and $\varphi(\frac{\nu_D}{T})$ is given by

$$\varphi\left(\frac{\nu_D}{T}\right) = \frac{k_B T}{h\nu_D}\int_0^{\frac{k_B T}{h\nu_D}}\left[\frac{x}{e^x-1}\right]dx \quad (2)$$

The $(36.39k_B)/(Mh\nu_D)$ parameter is related to the ground state energy. According to Ref. [25], we include into Eq. (1) an additional refinable term B_{static} corresponding to the sum of static components of the experimental temperature factor and uncorrected systematic errors. The symbols in Fig. 4 represent the experimental B_{iso} obtained from neutron diffraction data together with error bars plotted versus temperature, while the model curves included in the plot correspond to the least-squares fit results from Eqs. (1) and (2). We recalculated the characteristic Debye frequency to the temperature scale and the following parameters were obtained for all atomic species: $\Theta_D^W = 172(5)$ K and $B_{static}^W = 0.19$ Å^2, $\Theta_D^{Pb} = 141(5)$ K and $B_{static}^{Pb} = 0.08$ Å^2, $\Theta_D^O = 438(5)$ K and $B_{static}^O = 0.32$ Å^2. The averaged mass-weighted value for the Debye temperature was derived from the characteristic vibrational frequencies and is equal to 195 ± 15 K.

3.2. Heat capacity and Debye temperature

The experimental heat capacity for $PbWO_4$ as a function of temperature is displayed in Fig. 5. No indications for any phase

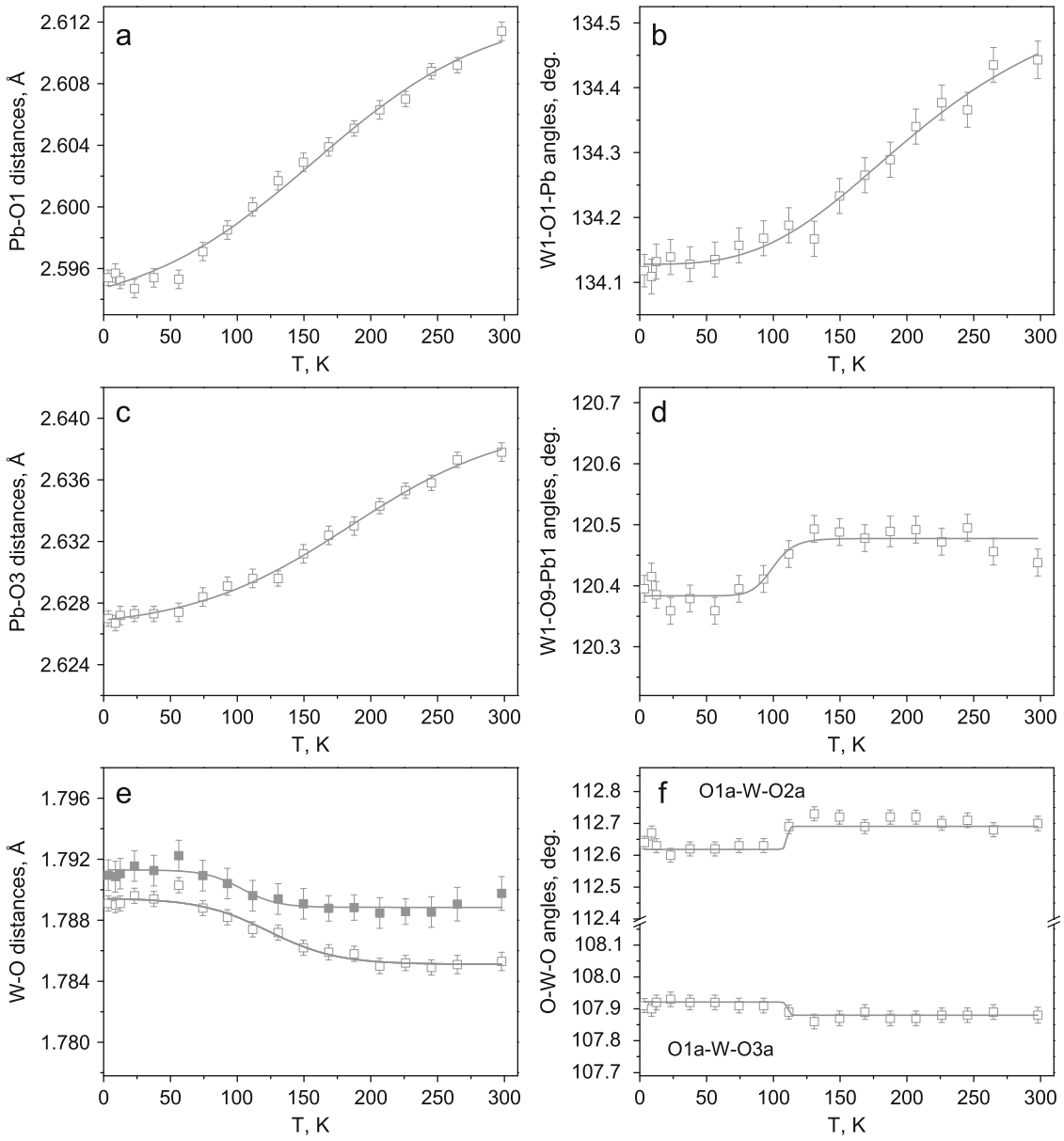

Fig. 3. Temperature dependencies of selected interatomic distances and angels of $PbWO_4$. Lines in all dependencies are sigmoidal fits to the data and are presented as guides to the eye. Empty and filled symbols in W–O vs. T plot represent observed and thermally corrected W–O distances in stolzite.

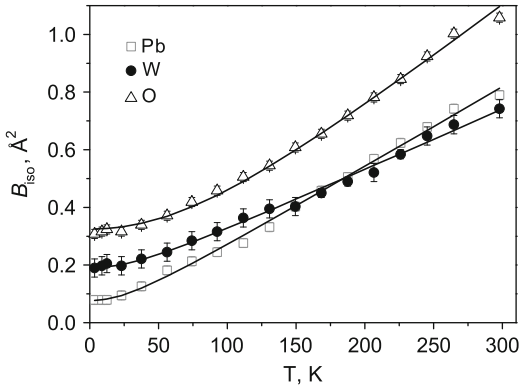

Fig. 4. Isotropic atomic displacement parameters of $PbWO_4$ obtained from neutron diffraction as functions of temperature: symbols with error bars show experimental data while solid lines correspond to fits to the data using Eqs. (1)–(2).

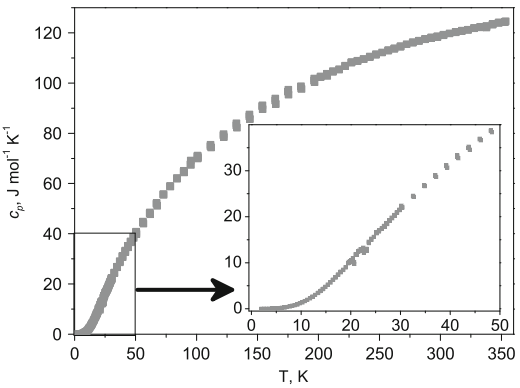

Fig. 5. Experimental heat capacity $c_p(T)$ of $PbWO_4$.

transformations were observed in the temperature range of 2.0–353.5 K. Assuming that the isobaric specific heat $c_p(T)$ is approximately equal to the isochoric value $c_v(T)$ at low temperatures, the Debye temperature was derived from the low temperature specific heat on the basis of a Debye approximation for heat capacity equaling the value of 237(8) K. Using a second approach, a Debye temperature of 237 K was calculated from the experimentally determined sound velocities (elastic moduli) [26] using the equations proposed by Robie and Edwards [27] which is in perfect agreement with our value derived from the heat capacity. This is quite surprising, because significant differences between "elastic" and "thermal" Debye temperatures were recently reported for the scheelite structured $CaWO_4$ [15] and $CaMoO_4$ [28]. Note that the value for the Debye temperature of 195(15) K from the analysis of the atomic displacement parameters differs by 19% from the "elastic" and "thermal" Debye temperatures which can be readily explained by the low accuracy in the determination of atomic displacement parameters from powder diffraction experiments.

3.3. Thermal expansion

Fig. 6 illustrates the temperature dependencies of the unit-cell dimensions of $PbWO_4$. The thermal expansions of the two crystallographic axes of $PbWO_4$ are positive and change without anomalies throughout the investigated temperature range. The volume thermal expansion was therefore parameterized in the framework of a 1st order Grüneisen approximation using the Debye model for the internal energy. Such a description of the thermal expansion in the low temperature range was shown to be appropriate even for a number of non-Debye-like

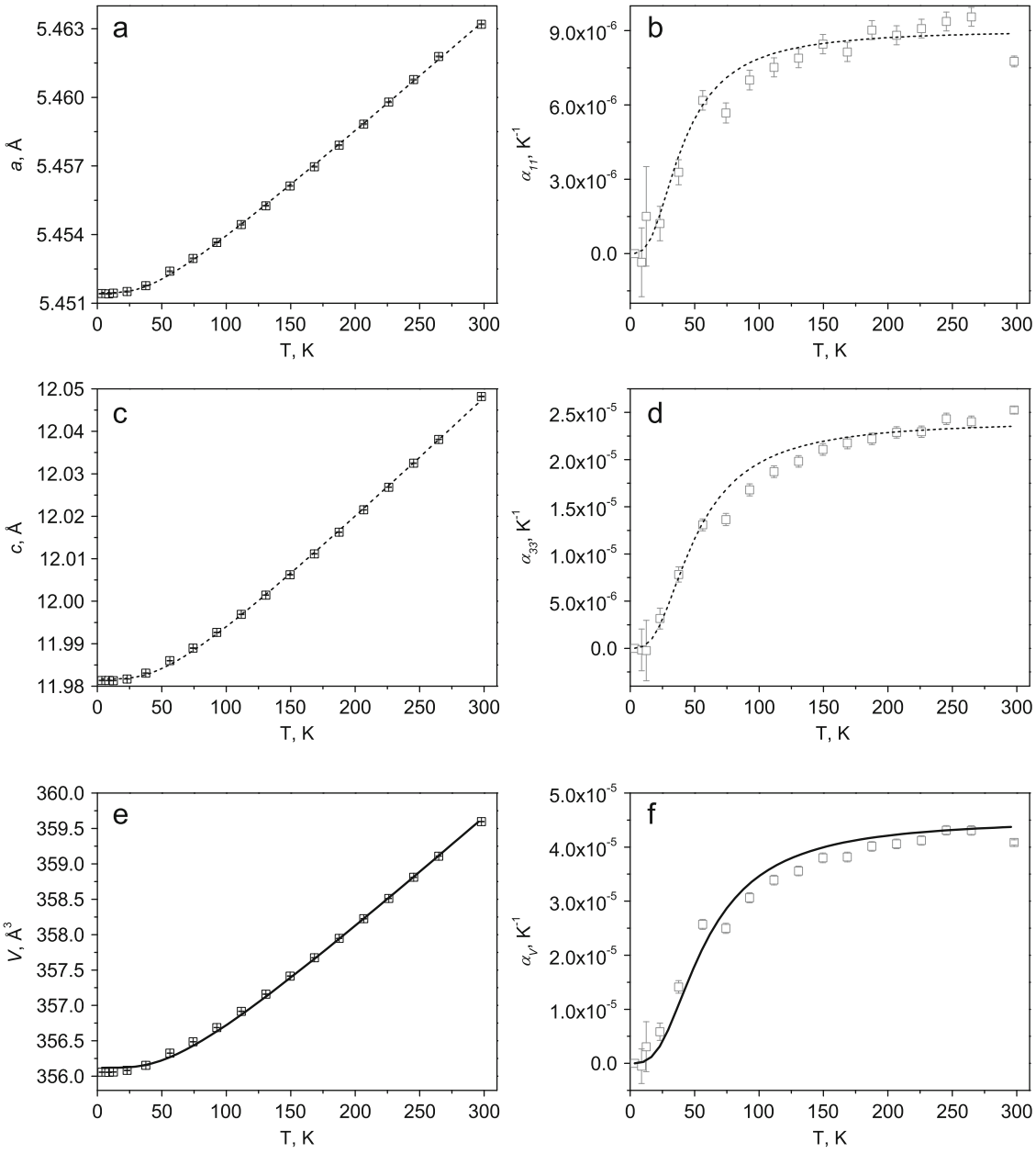

Fig. 6. The unit cell dimensions and thermal expansion coefficients of $PbWO_4$. Symbols are either experimental data of cell dimensions obtained from Rietveld refinements or their numerical differentiation. Solid lines correspond to fits according Eqs. (3), (4) for $V(T)$ and $\alpha_V(T)$ dependencies, dashed lines are guides to the eye in other dependencies.

compounds (see for example recent works [29–31] and references therein). Assuming the Grüneisen parameter γ and the bulk modulus K to be temperature independent, the thermal evolution of the cell volume at low temperatures can be described as

$$V(T) = V_0 + \frac{\gamma}{K}U(T) = V_0 + \frac{\gamma}{K}\left[9Nk_BT\left(\frac{T}{\Theta_D}\right)^3\int_0^{\frac{\Theta_D}{T}}\frac{x^3\,dx}{e^x-1}\right] \quad (3)$$

where V_0 is volume at 0 K and N is number of atoms per unit cell. We have fitted V_0 and γ in Eq. (3) to the experimentally determined volume *versus* temperature dependency. For the fit, the "thermal" Debye temperature of $\Theta_D = 237$ K and the bulk modulus $K = 67$ GPa were used. The mean bulk modulus of 67 GPa is the average from results of high-pressure diffraction experiments 64(2) GPa [19], 66(5) GPa [20] and from the tensor of elastic constants determined by sound velocity measurements in [26] using the Reuss–Voight–Hill averaging scheme [32], 71 GPa. Using the refined parameters $V_0 = 356.911$ Å^3 and $\gamma = 1.08$ obtained from fitting the temperature dependence of the volume, we calculated the magnitude of the volumetric thermal expansion coefficients as a function of temperature using following expression:

$$\alpha_V(T) = \frac{\partial \ln[V(T)]}{\partial T} \quad (4)$$

The volumetric thermal expansion coefficient α_V derived from Eqs. (3)–(4) in the range of 3.5–300 K range is presented together with the points obtained from the numerical differentiation of the lattice dimensions in Fig. 6. On the other hand, the components of the thermal expansion tensor α_{11} and α_{33} were obtained from the numerical differentiation of the cell dimensions and the lines through the experimental points are guides to the eye (Fig. 6). Comparing our averaged values of $38(1)\times10^{-6}$ and $40.3(3)\times10^{-6}$ K^{-1} for the thermal expansion coefficients α_{11} and α_{33} over the temperature ranges 100–200 and 200–300 K, respectively, with those of 40.5×10^{-6} and 49.2×10^{-6} K^{-1} over the same ranges from Ref. [10], the difference of 20% over 200–300 K is obvious. Such a pronounced discrepancy can mainly be attributed to the use of different parameterizing functions for the thermal expansion: usual polynomial functions do not adequately describe the thermal expansion at low temperatures (especially in the case of limited data sets). Furthermore, it does not make sense to compare data derived from two data points [9]. The anisotropy of the thermal expansion in $PbWO_4$ at low temperatures is apparent: despite the similar temperature behaviour of α_{11} and α_{33}, the crystal expands along the c-axis about 2.53 times higher in comparison to the expansion along the a-axis. This is consistent with results of [9,12,10] and, in particular, with Ref. [11], where the large anisotropy of the thermal expansion with $\alpha_c/\alpha_a \sim 2.3$ at high temperatures were revealed. The structural origin of this anisotropic behaviour of the thermal expansion is readily attributed to the following feature of the $PbWO_4$ crystal structure: similar to the anisotropic compressibility [19,20,23], the expansivity along the a-axis is lower than along the c-axis because rigid WO_4^{2-} units are arranged along the $\langle 100\rangle$−directions while Pb^{2+} cations occupy sites between WO_4^{2-} in the $\langle 001\rangle$−directions. Therefore, the lower expansivity of the a-axis arises from the orientation of shared edges between PbO_8 polyhedra, which lie close to the (001) plane and, consequently, restrict the expansivity perpendicular to the c-axis (i.e. along the a-axis).

4. Conclusions

The temperature variations of the Pb–O distances are more pronounced in comparison to the tiny temperature induced changes of the rigid tetrahedral W–O lengths which therefore mainly determines the magnitude of the thermal expansion. The angles O–W–O within the tetrahedra and the smaller interpolyhedral angles W–O–Pb do not significantly depend on temperature, whereas the larger interpolyhedral angles W–O–Pb increase more significantly upon increasing temperature. A distinct feature of the temperature induced structural variations in $PbWO_4$ are the different expansivities of shorter and longer Pb–O distances, which implies the possible influence of "nonbonded" lone-pair of the Pb^{2+} ion on the structural variations.

The low temperature thermal expansion reveals no anomalies and was parameterized on the basis of a 1st order Grüneisen approximation with a Debye approximation for an internal energy with $\Theta_D = 237$ K, $K = 67$ GPa, $V_0 = 356.911$ Å^3 and $\gamma = 1.08$. In analogy with the anisotropic compressibility stated in [19,20] and [23], the lower thermal expansion along the a-axis of $PbWO_4$ arises from the fact that rigid tetrahedral units are arranged along the $\langle 100\rangle$−directions, while Pb^{2+} cations occupy sites between WO_4^{2-} in the $\langle 001\rangle$−directions. Such a pronounced anisotropic behaviour is a crucial issue which has to be accounted for in the design of $PbWO_4$-based devices for operation in cryogenic environments.

Acknowledgments

FRM II is gratefully acknowledged for allocation of the beamtime. We are also extremely grateful to Dr. Andrzej Grzechnik, Dr. Thomas Vad and Dr. Daniel J. Frost for discussions and help in the preparation of the manuscript.

Appendix A. Supplementary data

Supplementary data associated with this article can be found in the online version at doi:10.1016/j.jssc.2010.03.039.

References

[1] R.M. Brown, Nucl. Instrum. Methods Phys. Res., Sect. A 57 (2007) 29–32.
[2] M. Ryan, Nucl. Instrum. Methods Phys. Res., Sect. A 598 (2009) 217–219.
[3] P.A. Semenov, Yu.V. Kharlov, A.V. Uzunian, S.K. Chernichenko, A.A. Derevschikov, A.M. Davidenko, Y.M. Goncharenko, V.A. Kachanov, A.S. Konstantinov, V.A. Kormilitsin, Yu.A. Matulenko, A.P. Meschanin, Y.M. Melnick, N.G. Minaev, V.V. Mochalov, D.A. Morozov, R.W. Novotny, A.A. Ryazantsev, A.P. Soldatov, L.F. Soloviev, V.G. Vasilchenko, A.N. Vasiliev, A.E. Yakutin, O.P. Yushchenko, Nucl. Instrum. Methods Phys. Res., Sect. A 598 (2009) 224–228.
[4] N. Akchurin, M. Alwarawrah, A. Cardini, G. Ciapetti, R. Ferrari, S. Franchino, M. Fraternali, G. Gaudio, J. Hauptman, F. Lacava, L. La Rotonda, M. Livan, M. Mancino, E. Meoni, H. Paar, D. Pinci, A. Policicchio, S. Popescu, G. Susinno, Y. Roh, W. Vandelli, T. Venturelli, C. Voena, I. Volobouev, R. Wigmans, Nucl. Instrum. Methods Phys. Res., Sect. A 593 (2009) 530–538.
[5] D. Millers, L. Grigorjeva, S. Chernov, A. Popov, P. Lecoq, E. Auffray, Phys. Status Solidi B 203 (1997) 585–589.
[6] P. Lecoq, I. Dafinei, E. Auffray, M. Schneegans, M.V. Korzhik, O.V. Missevitch, V.B. Pavlenko, A.A. Fedorov, A.N. Annenkov, V.L. Kostylev, V.D. Ligun, Nucl. Instrum. Methods Phys. Res., Sect. A 365 (1995) 291–298.
[7] J.M. Moreau, P. Galez, J.P. Peigneux, M.V. Korzhik, J. Alloys Compd. 238 (1996) 46–48.
[8] J.M. Moreau, R.E. Gladyshevskii, P. Galez, J.P. Peigneux, M.V. Korzhik, J. Alloys Compd. 284 (1999) 104–107.
[9] R. Chipaux, G. André, A. Cousson, J. Alloys Compd. 325 (2001) 91–94.
[10] T. Beguemsi, P. Garnier, D. Weigel, J. Solid State Chem. 25 (1978) 315–324.
[11] M. Ishii, K. Harada, M. Kobayashi, Y. Usuki, T. Yazawa, Nucl. Instrum. Methods Phys. Res., Sect. A 376 (1996) 203–207.
[12] A.P. Eremenko, N.B. Kofanova, L.E. Pustovaya, A.G. Rudskaya, B.S. Kul'buzhev, M.F. Kupriyanov, Phys. Solid State 46 (2004) 1914–1916.
[13] M. Hoelzel, A. Senyshyn, R. Gilles, H. Boysen, H. Fuess, Neutron News 18 (4) (2007) 23–26.
[14] ⟨http://www.ill.eu/sites/fullprof/index.html⟩.
[15] A. Senyshyn, H. Kraus, V. Mikhailik, V. Yakovyna, Phys. Rev. B 70 (21) (2004) 214306.

[16] S.N. Achary, S.J. Patwe, M.D. Mathews, A.K. Tyagi, J Phys. Chem. Solids 67 (2006) 774–781.
[17] J.S.O. Evans, T.A. Mary, T. Vogt, M.A. Subramanian, A.W. Sleight, Chem. Mater. 8 (1996) 2809–2823.
[18] R.T. Downs, in: R.M. Hazen, R.T. Downs (Eds.), High-Temperature and High-Pressure Crystal Chemistry, Reviews in Mineralogy and Geochemistry, vol. 41, The Mineralogical Society of America, Washington, 2000, pp. 61–87.
[19] A. Grzechnik, W.A. Crichton, W.G. Marshall, K. Friese, J. Phys. Condens. Matter 18 (2006) 3017–3029.
[20] D. Errandonea, J. Pellicer-Porres, F.J. Manjón, A. Segura, Ch. Ferrer-Roca, R.S. Kumar, O. Tschauner, J. López-Solano, P. Rodríguez-Hernández, S. Radescu, A. Mujica, A. Muñoz, G. Aquilanti, Phys. Rev. B 73 (2006) 224103.
[21] A. Senyshyn, L. Vasylechko, H. Boysen, H. Ehrenberg, M. Hoelzel, T. Hansen, H. Fuess, Thermal expansion and atomic vibrations in $CaWO_4$ studied by neutron and synchrotron powder diffraction, in Materials of 23rd European Crystallographic Meeting ECM23 (Leuven, Belgium, 2006), Acta Crystallogr., Sect. A: Found. Crystallogr. 62 (2006) s117.
[22] A. Senyshyn, L. Vasylechko, R. Mole, M. Hoelzel, T.C. Hansen, V. Mikhailik, H. Fuess, Thermal expansion and atomic vibrations in $CaWO_4$ studied by neutron and synchrotron powder diffraction, Deutsche Neutronenstreutagung 2008, Garching b. Munchen, Germany, 14–17 September, 2008, Program & Collected Abstracts, p. 76.
[23] R.M. Hazen, L.W. Finger, J.W.E. Mariathasan, J. Phys. Chem. Solids 46 (1985) 253–263.
[24] K. Lonsdale, C.H. MacGillavry, G.D. Riek, International Tables for X-ray Crystallography, vol. III, Kynoch Press, Birmingham, 1962, p. 232.
[25] D.N. Argyriou, J. Appl. Crystallogr. 27 (1994) 155–158.
[26] N.P. Kobelev, Y.M. Soifer, Fizika Tverdogo Tela 38 (1996) 3589–3594 in Russian.
[27] R.A. Robie, J.L. Edwards, J. Appl. Phys. 37 (1966) 2659–2663.
[28] A. Senyshyn, H. Kraus, V.B. Mikhailik, L. Vasylechko, M. Knapp, Phys. Rev. B 73 (2006) 014104.
[29] A.D. Fortes, I.G. Wood, L. Vočadlo, H.E.A. Brand, K.S. Knight, J. Appl. Crystallogr. 40 (2007) 761–770.
[30] D.M. Trots, A. Senyshyn, L. Vasylechko, R. Niewa, T. Vad, V.B. Mikhailik, H. Kraus, J. Phys. Condens. Matter 21 (2009) 325402.
[31] A. Senyshyn, D.M. Trots, J.M. Engel, L. Vasylechko, H. Ehrenberg, T. Hansen, M. Berkowski, H. Fuess, J. Phys. Condens. Matter 21 (2009) 145405.
[32] P. Belikov, K.S. Aleksandrov, T.V. Ryzhova, Elastic Constants of Rock-Forming Minerals, Nauka, Moscow, 1970 (in Russian).